2021 IEEE 18th International Symposium on Biomedical Imaging (ISBI)
April 13-16, 2021, Nice, France

NON-RIGID REGISTRATION OF LIVE CELL NUCLEI USING GLOBAL OPTICAL FLOW WITH ELASTICITY CONSTRAINTS

Qi Gao[1], Vadim O. Chagin[2,3], M. Cristina Cardoso[2], and Karl Rohr[1]

[1]Biomedical Computer Vision Group, BioQuant, IPMB, Heidelberg University and DKFZ, Germany
[2]Cell Biology and Epigenetics, Department of Biology, Technical University of Darmstadt, Germany
[3]Institute of Cytology, Russian Academy of Sciences, St. Petersburg, Russia

ABSTRACT

Non-rigid registration of cell nuclei in time-lapse microscopy images requires the estimation of nucleus deformation. We propose a new approach for deformation estimation and non-rigid registration of cell nuclei, which integrates elasticity constraints into a global optical flow-based method. We derive an elasticity prior on the deformation from the Navier equation. The common Markov random field prior in previous global methods is replaced by the elasticity prior to better regularize the estimated deformation fields. In addition, we introduce a scheme to exclude sub-cellular structures from estimating the nucleus deformation so that their relative motion does not deteriorate the registration result. Experiments on live cell microscopy image data demonstrate that the proposed method with elasticity constraints outperforms previous methods.

Index Terms— Non-rigid Registration, Elasticity, Fluorescence Microscopy Images.

1. INTRODUCTION

Live cell time-lapse microscopy allows analyzing the dynamics of sub-cellular structures (*e.g.*, proteins) to better understand cellular processes and functions. As the motion of sub-cellular structures is superimposed on the deformation and motion of cell nuclei, registration of cell nuclei is needed to decouple the two types of motion. Generally, non-rigid registration methods are required to cope with cell nucleus deformation.

In previous work on non-rigid registration of cell nuclei, often intensity-based methods were used since changes of image intensity are direct evidence for estimating motion and deformation. In [1], a polynomial optical flow model was introduced to estimate cell motion. [2, 3] and [4] use local and global optical flow models, respectively, to compute the deformation fields of nuclei with an incremental scheme. However, these methods are not based on an elasticity model to accurately determine cell deformation.

Elasticity properties of cells were studied in [5]. It was found that the intranuclear region is stiffer and more elastic than the cytoplasm. For non-rigid registration of cell nuclei, contour-based methods that exploit elasticity properties were proposed. In [6], the deformation of the nuclear contour is determined from the image data, and deformation vectors inside the nucleus are interpolated using polyharmonic splines. Linear elasticity was explicitly modeled in [7] and combined with contour matching. Final deformation fields are interpolated using thin-plate splines or partial differential equations. However, in [6, 7] deformation estimation only depends on the nucleus contours, while image intensity information is not directly exploited. Thus, local deformations inside the cell nucleus cannot be captured.

In this paper, we propose a new non-rigid registration method for cell nuclei in live cell microscopy data, which integrates elasticity constraints in a global probabilistic optical flow-based model. We analyze the Navier equation from linear elasticity theory and derive an elasticity prior term. The likelihood term is modeled based on image intensities. We also introduce a scheme to exclude sub-cellular structures from estimating the deformation so that their relative motion does not deteriorate the registration result. Compared to previous contour-based methods for non-rigid registration that use an elasticity model [7], our method exploits intensity changes inside cell nuclei that act as body forces and provide additional information. Experiments using real cell microscopy images demonstrate that the proposed method outperforms previous methods.

2. METHODS

2.1. From elasticity theory to an elasticity prior

In linear elasticity theory, the deformation field (displacement vector field) $\mathbf{w}$ for isotropic and homogeneous material can be determined by solving the Navier equation given the body forces $\mathbf{f}$ [8]:

$$\mu\nabla^2\mathbf{w} + (\lambda+\mu)\nabla(\nabla\cdot\mathbf{w}) + \mathbf{f} = 0, \qquad (1)$$

where μ and λ are the Lamé constants, and ∇ is the nabla operator.

To derive an elasticity prior that is consistent with (1), we consider an energy function of a 2D deformation field $\mathbf{w} \in \mathbb{R}^{2N}$ (N is the number of pixels in an image) and the given forces $\mathbf{f} \in \mathbb{R}^{2N}$

$$E(\mathbf{w};\mathbf{f}) = -\mathbf{f}^{\mathrm{T}}\mathbf{w} + \frac{1}{2}\mu s + \frac{1}{2}(\lambda+\mu)t, \tag{2}$$

$$\text{with} \quad s = \|\mathbf{D}_x\mathbf{u}\|^2 + \|\mathbf{D}_y\mathbf{u}\|^2 + \|\mathbf{D}_x\mathbf{v}\|^2 + \|\mathbf{D}_y\mathbf{v}\|^2, \tag{3}$$

$$t = \|\mathbf{D}_x\mathbf{u} + \mathbf{D}_y\mathbf{v}\|^2. \tag{4}$$

Here $\mathbf{u} \in \mathbb{R}^N$ and $\mathbf{v} \in \mathbb{R}^N$ are x- and y-components of $\mathbf{w}$, respectively, $\mathbf{D}_x$ and $\mathbf{D}_y$ are matrices for computing the first order partial derivatives of $\mathbf{u}$ and $\mathbf{v}$ in x- and y-direction, and $\|\cdot\|$ is the ℓ_2 norm. The necessary condition for the minimization of (2) is

$$\begin{aligned} \mathbf{0} &= \nabla_{\mathbf{w}} E(\mathbf{w};\mathbf{f}) \\ &= -\mathbf{f} + \mu \begin{bmatrix} \mathbf{D}_x^{\mathrm{T}}\mathbf{D}_x + \mathbf{D}_y^{\mathrm{T}}\mathbf{D}_y & \mathbf{0} \\ \mathbf{0} & \mathbf{D}_x^{\mathrm{T}}\mathbf{D}_x + \mathbf{D}_y^{\mathrm{T}}\mathbf{D}_y \end{bmatrix} \begin{bmatrix} \mathbf{u} \\ \mathbf{v} \end{bmatrix} \\ &\quad + (\lambda+\mu) \begin{bmatrix} \mathbf{D}_x^{\mathrm{T}}\mathbf{D}_x & \mathbf{D}_x^{\mathrm{T}}\mathbf{D}_y \\ \mathbf{D}_y^{\mathrm{T}}\mathbf{D}_x & \mathbf{D}_y^{\mathrm{T}}\mathbf{D}_y \end{bmatrix} \begin{bmatrix} \mathbf{u} \\ \mathbf{v} \end{bmatrix} \\ &= -\mathbf{f} - \mu \begin{bmatrix} \mathbf{u}_{xx} + \mathbf{u}_{yy} \\ \mathbf{v}_{xx} + \mathbf{v}_{yy} \end{bmatrix} - (\lambda+\mu) \begin{bmatrix} \mathbf{u}_{xx} + \mathbf{v}_{yx} \\ \mathbf{u}_{xy} + \mathbf{v}_{yy} \end{bmatrix}, \end{aligned} \tag{5}$$

where double subscripts of $\mathbf{u}$ and $\mathbf{v}$ denote second order partial derivatives. Since (5) is equivalent to (1), linear elasticity is included in the energy function in (2) to model the displacements given body forces. We can accordingly establish a probabilistic posterior model of displacements under linear elasticity in a Bayesian framework with a likelihood term

$$p(\mathbf{f}|\mathbf{w}) \propto \exp\{\mathbf{f}^{\mathrm{T}}\mathbf{w}\} \tag{6}$$

and an elasticity prior

$$p(\mathbf{w};\mu,\lambda) \propto \exp\{-\tfrac{1}{2}\mu s\} \cdot \exp\{-\tfrac{1}{2}(\lambda+\mu)t\}. \tag{7}$$

In (7), the first term is a common Gaussian Markov random field where the partial derivatives of $\mathbf{u}$ and $\mathbf{v}$ are assumed to be independent (*e.g.*, as in [4]), while the second term is a multivariate Gaussian coupling the partial derivatives of $\mathbf{u}$ in x-direction with the partial derivatives of $\mathbf{v}$ in y-direction.

2.2. Deformation estimation using the elasticity prior

We employ the derived elasticity prior in (7) to extend the global model under a Bayesian framework in [4] for estimating the deformation of nuclei. Given two consecutive frames $\mathbf{x}^{\circ}$ and $\mathbf{x}^{\imath}$, the likelihood term is modeled based on image intensities under a brightness constancy assumption

$$p(\mathbf{x}^{\circ}|\mathbf{w},\mathbf{x}^{\imath}) \propto \prod_i \exp\big\{-\frac{1}{\alpha_i}(\mathbf{x}_i^{\circ} - \mathbf{x}_{\mathbf{w}i}^{\imath})^2\big\}, \tag{8}$$

where i is the index of image pixel locations, α_i the regularization weight, and $\mathbf{x}_{\mathbf{w}}^{\imath}$ the warped image of $\mathbf{x}^{\imath}$ towards $\mathbf{x}^{\circ}$ by the deformation field $\mathbf{w}$. To handle the problem that the relative motion of sub-cellular structures deteriorates the estimation of nucleus deformation, we detect sub-cellular structures in the image data and ignore the corresponding pixels by setting $\alpha_i = \infty$. For the other pixels, we use an adaptive scheme (as in [4]) to determine the weights α_i and improve the robustness to noise and outliers.

For the regularization term, we employ the derived elasticity prior

$$p(\mathbf{w}) \propto \exp\{-\beta s\} \cdot \exp\{-\gamma t\}, \tag{9}$$

where $\beta = \frac{1}{2}\mu$ and $\gamma = \frac{1}{2}(\lambda+\mu)$ are model parameters, and s and t are defined in (3) and (4). Compared to the regularization term in [4], we have an extra term that penalizes the divergence of the deformation field.

Note that for both the likelihood term and regularization term, the penalizing functions have a quadratic form. A benefit is that the optimization is very efficient. In fact, in [4] it was found that a quadratic penalizer is better suited than non-convex functions which are often used for images of natural scenes. The reasons are due to the special characteristics of image noise in fluorescence microscopy images and the deformation of nuclei.

In our approach, the deformation field $\mathbf{w}$ between $\mathbf{x}^{\circ}$ and $\mathbf{x}^{\imath}$ is computed using the maximum a-posteriori (MAP) estimate of the posterior $p(\mathbf{w}|\mathbf{x}^{\circ},\mathbf{x}^{\imath}) \propto p(\mathbf{x}^{\circ}|\mathbf{w},\mathbf{x}^{\imath}) \cdot p(\mathbf{w})$. A first order Taylor expansion is used to linearize the likelihood term in (8) assuming small deformation. The MAP estimate can be obtained by solving the linear system of equations

$$\left(\begin{bmatrix} \mathbf{\Lambda}\mathbf{\Gamma}_{\mathbf{x}_x^{\imath}} \\ \mathbf{\Lambda}\mathbf{\Gamma}_{\mathbf{x}_y^{\imath}} \end{bmatrix} \begin{bmatrix} \mathbf{\Gamma}_{\mathbf{x}_x^{\imath}} \\ \mathbf{\Gamma}_{\mathbf{x}_y^{\imath}} \end{bmatrix}^{\mathrm{T}} + \beta \begin{bmatrix} \mathbf{F} & \mathbf{0} \\ \mathbf{0} & \mathbf{F} \end{bmatrix} + \gamma \begin{bmatrix} \mathbf{D}_x^{\mathrm{T}}\mathbf{D}_x & \mathbf{D}_x^{\mathrm{T}}\mathbf{D}_y \\ \mathbf{D}_y^{\mathrm{T}}\mathbf{D}_x & \mathbf{D}_y^{\mathrm{T}}\mathbf{D}_y \end{bmatrix} \right) \mathbf{w} = \begin{bmatrix} \mathbf{\Lambda}\mathbf{\Gamma}_{\mathbf{x}_x^{\imath}} \\ \mathbf{\Lambda}\mathbf{\Gamma}_{\mathbf{x}_y^{\imath}} \end{bmatrix} (\mathbf{x}^{\circ} - \mathbf{x}^{\imath}), \tag{10}$$

where $\mathbf{\Gamma}_{\mathbf{x}_x^{\imath}} = \mathrm{diag}(\mathbf{x}_x^{\imath})$ and $\mathbf{\Gamma}_{\mathbf{x}_y^{\imath}} = \mathrm{diag}(\mathbf{x}_y^{\imath})$ are diagonal matrices containing the first order partial derivatives of $\mathbf{x}^{\imath}$ in x- and y-direction, $\mathbf{\Lambda} = \mathrm{diag}([\cdots, {}^1\!/_{\alpha_i}, \cdots])$ represents the weights α_i, and $\mathbf{F} = \mathbf{D}_x^{\mathrm{T}}\mathbf{D}_x + \mathbf{D}_y^{\mathrm{T}}\mathbf{D}_y$. Solving (10) is very efficient since the coefficient matrix on the left side is sparse and positive definite. To deal with large deformations, we use a standard coarse-to-fine strategy.

2.3. Registration of cell nuclei in image sequences

To register all frames of a temporal image sequence to the first frame, we compute the deformation fields $\mathbf{w}^{t-1,t}, t = 1, 2, ...$, between all pairs of consecutive frames, and use an incremental scheme to construct the deformation field $\mathbf{w}^{0,t}$ for registration of frame $\mathbf{x}^t$ at time t to the first frame $\mathbf{x}^0$:

$$\mathbf{w}^{0,t} = \mathbf{w}^{0,t-1} \circ \mathbf{w}^{t-1,t}, \tag{11}$$

where the operator "$\circ$" denotes concatenation. The incremental scheme has the advantage that it better copes with the heterogeneous changes of the intensity structure over time in live cell microscopy images [4].

Table 1. Registration errors (in pixel) for annotated feature points in image sequences of dataset A.

Sequence	A1				A2			
Annotator	H_1	H_2	H_3	Avg.	H_1	H_2	H_3	Avg.
Unregistered	30.17	30.75	31.29	30.74	49.42	50.20	49.05	49.55
Contour-based method [7] (elasticity static)	5.96	7.20	6.01	6.39	8.23	9.45	8.97	8.89
Contour-based method [7] (elasticity dynamic)	5.71	7.18	5.78	6.22	7.95	9.10	8.78	8.61
Optical flow-based method [4] (brightness features)	6.69	7.42	5.38	6.50	7.19	7.85	7.80	7.61
Optical flow-based method [4] (high-order features)	5.98	6.81	3.93	5.57	6.45	6.78	7.86	7.03
Proposed method (with elasticity constraints)	**5.36**	**5.29**	**3.75**	**4.80**	**5.63**	**6.62**	**6.67**	**6.31**

3. EXPERIMENTS

Data. For a quantitative evaluation of our proposed method we use two datasets of live cell microscopy image sequences. Dataset A consists of two sequences of U2OS cell nuclei stained with mCherry-BP1-2 and UV-irradiated in a stripe-like region: (A1) 25 frames and (A2) 38 frames of 512×512 pixels, which were acquired by a confocal microscope with a resolution of $240.5\text{nm}\times240.5\text{nm}$ [9]. Feature points in the UV-irradiated strips were manually tracked by three independent annotators. This dataset has been used in [7] and [4] for evaluation. Dataset B is an image sequence including 10 frames of 350×350 pixels generated by a confocal microscope with a resolution of $104\text{nm}\times104\text{nm}$, showing replication foci (expressed by fluorescently tagged PCNA) in nuclei of HeLa cells during S-Phase [10].

Implementation details. The model parameters β and γ in (9) were optimized by first choosing a suitable value for β, and then setting γ empirically to $5\sim10$ times larger than β. For dataset B, to exclude replication foci from deformation estimation, we used a Laplacian-of-Gaussian (LoG) spot detector with $\sigma=2$ to locate foci. For all pixels with a distance of no more than 5 pixels to detected foci, α_i in (8) was set to ∞. For the coarse-to-fine strategy, 5 and 4 image scales were used for datasets A and B, respectively.

3.1. Performance evaluation and comparison

Due to significant noise as well as appearing and disappearing sub-cellular structures in the considered microscopy images, a direct comparison (*e.g.*, of the image intensities) between the reference frame and the registered frames does not properly quantify the registration accuracy. Thus, for both sequences in dataset A, we exploit manually annotated feature points and compute the geometric registration error defined as the Euclidean distance of each feature point in the registered image to its corresponding location in the reference image.

We compared the registration results of the proposed method with those of the contour-based method [7] which also includes an elasticity model (static or dynamic) and the global optical flow method in [4] (brightness features or high-order features). The results are provided in Tab. 1. It can be seen that the registration error of the proposed method with elasticity constraints is much lower than that of the previous methods. We attribute this to the fact that the proposed method exploits intensity information inside cell nuclei to capture local deformation. Note that the proposed method uses only brightness information but outperforms the previous model [4] using learned high-order features. This demonstrates that it is important to use an elasticity model for registration. Fig. 1 shows the registration result of the proposed method for sequence A2 illustrated by the distribution of feature points in all 38 frames of the sequence from one annotator. It can be seen that the variation of the feature points in the registered images is much smaller.

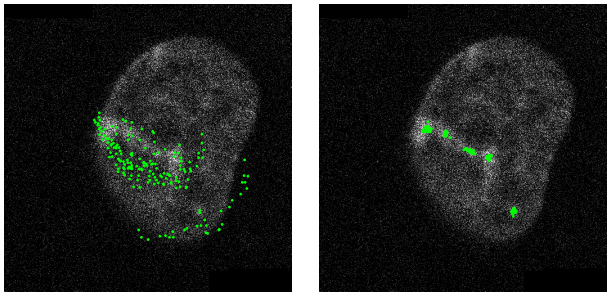

Fig. 1. Example registration result. Distribution of feature points in all 38 frames of sequence A2 from one annotator, overlaid with the 1st frame. *(Left)* unregistered; *(Right)* registered by the proposed method.

For dataset B, it is very difficult to define corresponding feature points for evaluation due to appearing and disappearing foci structures. However, there exist hole structures inside cell nuclei (nucleoli), which can be straightforwardly annotated (Fig. 2(b)). Exploiting the warped annotations of nucleoli in the registered images (Fig. 2(c,d)), the registration accuracy can be quantified. For a comparison, we computed the area of the nucleoli. The results are shown in Fig. 3. It can be seen that the proposed method with elasticity constraints much better preserves the size of the nucleoli in the registered images compared to the previous method [4].

The computation time of the proposed method with elasticity constraints is only a little bit higher than that of the previous global method [4] (*e.g.*, 1min 32sec *vs.* 1min 20sec for registration of sequence A2 on a Linux PC with an Intel

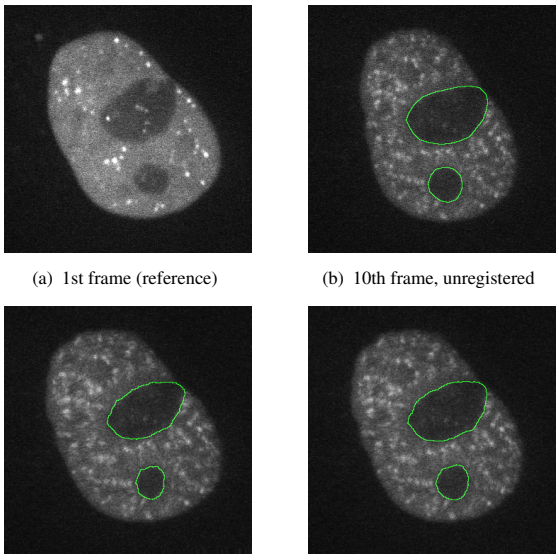

(a) 1st frame (reference) (b) 10th frame, unregistered

(c) 10th frame registered by method [4] (d) 10th frame registered by the proposed method

Fig. 2. Registration results of the 1st and 10th frame of dataset B. Green contours indicate nucleoli inside the nucleus in the unregistered and registered frames.

Core i9 3.60GHz CPU). The reason is that the coefficient matrix of the linear system of equations in (10) is slightly less sparse. As the deformation fields between all pairs of consecutive frames are estimated independently, parallelization is straightforward and can be used to further reduce the computation time.

4. SUMMARY

We introduced a new non-rigid registration method for cell nuclei in time-lapse microscopy data, which integrates elasticity constraints in a global optical flow-based model. This was achieved by including an elasticity prior based on the Navier equation in the deformation estimation model. We also proposed a scheme to exclude sub-cellular structures from estimating the nucleus deformation so that their relative motion does not deteriorate the registration result. Experiments demonstrated that the proposed approach outperforms a previous global optical flow-based method and a contour-based method.

Compliance with Ethical Standards. This work is a study for which no ethical approval was required.

Acknowledgement. Support of the DFG within the SPP 2202 (RO 2471/10-1, CA 198/15-1) as well as CA 198/9-2, and the BMBF project de.NBI (031A537C, HD-HuB) is acknowledged.

5. REFERENCES

[1] S. Ozere, P. Bouthemy, F. Spindler, P. Paul-Gilloteaux, and C. Kervrann, "Robust parametric stabilization of moving cells with intensity correction in light microscopy image sequences," in *Proc. IEEE Int. Symp. on Biomed. Imag. (ISBI)*, 2013, pp. 468–471.

[2] I. Kim, Y. M. Chen, D. L. Spector, R. Eils, and K. Rohr, "Nonrigid registration of 2-D and 3-D dynamic cell nuclei images for improved classification of subcellular particle motion," *IEEE Trans. Image Process.*, vol. 20, no. 4, pp. 1011–1022, 2011.

[3] M. Tektonidis and K. Rohr, "Diffeomorphic multi-frame non-rigid registration of cell nuclei in 2D and 3D live cell images," *IEEE Trans. Image Process.*, vol. 26, no. 3, pp. 1405–1417, 2017.

[4] Q. Gao and K. Rohr, "A global method for non-rigid registration of cell nuclei in live cell time-lapse images," *IEEE Trans. Med. Imag.*, vol. 38, no. 10, pp. 2259–2270, 2019.

[5] Y. Tseng, J. S. H. Lee, T. P. Kole, I. Jiang, and D. Wirtz, "Micro-organization and visco-elasticity of the interphase nucleus revealed by particle nanotracking," *J. Cell Sci.*, vol. 117, pp. 2159–2167, 2004.

[6] J. De Vylder, W. H. De Vos, E. M. Manders, and W. Philips, "2D mapping of strongly deformable cell nuclei based on contour matching," *Cytometry Part A*, vol. 79A, pp. 580–588, 2011.

[7] D. V. Sorokin, I. Peterlik, M. Tektonidis, K. Rohr, and P. Matula, "Non-rigid contour-based registration of cell nuclei in 2-D live cell microscopy images using a dynamic elasticity model," *IEEE Trans. Med. Imag.*, vol. 37, no. 1, pp. 173–184, 2018.

[8] M. H. Sadd, *Elasticity: Theory, Applications, and Numerics*, 3rd ed. Elsevier, 2014.

[9] V. Foltankova, P. Matula, D. V. Sorokin, S. Kozubek, and E. Bartova, "Hybrid detectors improved time-lapse confocal microscopy of PML and 53BP1 nuclear body colocalization in DNA lesions," *Microscopy and Microanalysis*, vol. 19, no. 2, pp. 360–369, 2013.

[10] V. O. Chagin, C. S. Casas-Delucchi, M. Reinhart *et al.*, "4D Visualization of replication foci in mammalian cells corresponding to individual replicons," *Nature Communications*, vol. 7, no. 11231, 2016.

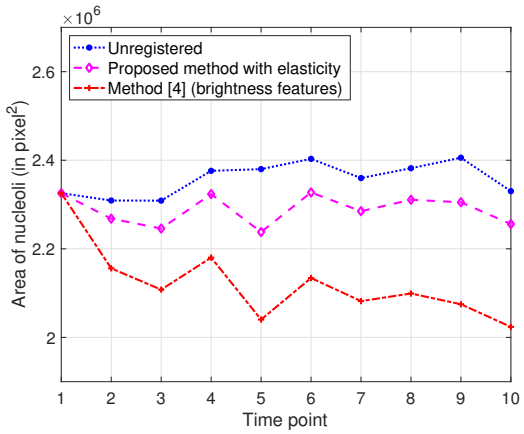

Fig. 3. Quantified area of nucleoli in the registered images of dataset B.